Hydrogen gas ameliorates the LPS-induced BPD via inhibiting the activation of TNF-α/NF-κB inflammatory signaling pathway in placenta

Yafang Zhang
The Affiliated Taian City Central Hospital of Qingdao University
Xianhui Ren
The Affiliated Taian City Central Hospital of Qingdao University
Linli Zhang
The Affiliated Taian City Central Hospital of Qingdao University
Xiujie Jing
The Affiliated Taian City Central Hospital of Qingdao University
Yunxi Chen
Tongji University Affiliated East Hospital
Yan Tian
Tongji University Affiliated East Hospital
Zhongxia Chu
The Affiliated Taian City Central Hospital of Qingdao University
Guo Yao
The Affiliated Taian City Central Hospital of Qingdao University
Yan Wang (allen081226@126.com)
The Affiliated Taian City Central Hospital of Qingdao University

Research Article

Keywords: hydrogen, BPD, placenta, inflammation, TNF-α, NF-κB

Posted Date: November 3rd, 2022

DOI: https://doi.org/10.21203/rs.3.rs-2216294/v1

Abstract

Objective

To investigate the anti-inflammatory role of H_2 in LPS-induced BPD via regulating TNF-α/NF-κB signaling pathway in placenta.

Methods

We induced a neonatal rat model of BPD by injecting lipopolysaccharide (LPS, 1ug) into the amniotic fluid at embryonic day 16.5(E16.5). Treatment of 30% hydrogen gas for 4 hours/day with continuously 5days. We primarily analyzed the neonatal outcomes and then compared inflammatory levels from Control group (CON), LPS group (LPS) and LPS with H_2 inhalation group (LPS + H_2). TUNEL and Hematoxylin-Eosin (HE) staining were performed to evaluate inflammatory and apoptotic levels. We further used RNA sequencing and ELISA assay to examine differentially expressed proteins and mRNA levels of tumor necrosis factor-α (TNF-α), nuclear factor kappa-B (NF-κB) (p65), interleukin (IL)-6, IL-18, IL-1β, C-C motif chemokine ligand 2(CCL2) and C-X-C motif chemokine ligand 1(CXCL1). Bioinformatics analysis (GO and KEEG) of RNA-seq and correlation analysis were applied to clarify the mechanisms of H_2 anti-inflammatory effect on LPS-induced BPD.

Results

We found the H_2 inhalation decreased production of inflammatory cytokines/chemokines (IL-6, IL-18, IL-1β, CCL2, CXCL1) in LPS-induced placenta to rescue from the BPD. Upon administration of H_2, infiltration degree of LPS-induced placenta was reduced and infiltrating significantly narrowed down. Hydrogen normalized LPS-induced perturbed lung development, reduced lung apoptotic index, death ratio of fetus and neonate. Meanwhile, H_2 also upregulated the survival ratio. RNA-seq and Elisa demonstrated that both mRNA and protein levels of TNF-α/NF-κB signaling pathway were activated by LPS, and H_2 relieved the pro-inflammatory function of LPS on TNF-α/NF-κB-stimulated placenta. Correlation analysis showed a positive association of TNF-α vs both NF-κB and inflammatory cytokines/chemokines.

Conclusion

H_2 inhalation alleviated LPS-induced BPD by inhibiting excessive pro-inflammatory cytokines and inflammatory chemokines via the TNF-α/NF-κB signaling pathway in placenta and may be a potential therapeutic strategy for BPD.

Introduction

Owing to lack of effective interventions to prevent preterm births and faced with life-saving postpartum intervention, BPD has been recognized as the most frequent complication in premature infants accompanied with high incidence and poor prognosis [1–3]. It can develop chronic lung dysfunction, persistent airway and pulmonary vascular diseases, seriously affect the quality in survival [4].

BPD is now considered as the result of an abnormal repair response to lung injury by multiple antenatal and postnatal exposures [5]. Inflammation, especially chorioamnionitis (CAM), is expressed as the common antenatal pathway that initiates the lung injury that can progress to a BPD phenotype [6]. The increasing evidence linking the inflammatory regulatory function in the placenta to BPD has been analyzed in a systematic review [7]. The placenta makes an adaptive response to CAM-induced by LPS [8], even placental histology is believed to predict adverse neonatal outcomes in some studies, which can cause the aggregation of placental decidual cells, amniotic cells and infiltrating macrophages and release pro-inflammatory cytokines and chemokines to the gestational sac [9], subsequently resulting in fetal inflammatory response syndrome (FIRS) and eventually contribute to the development of BPD [10, 11]. Concerning the vital role of placenta in anti-inflammation, it is conceivable that alterations of placenta can reverse the process LPS-induced BPD and result in improving the poor prognosis that has lifelong consequences.

Hydrogen, a novel therapeutic molecule, plays the biological effects by mainly anti-inflammatory, antioxidant and anti-apoptosis, which have been confirmed by many cellular, animal and clinical trials [12–14]. Despite many inaccuracies, inflammation scavenging ability is still the widely accepted mechanism of H_2 [15, 16]. Lack of any known adverse effects of hydrogen makes hydrogen an ideal anti-inflammatory therapeutic modality [17, 18]. Therefore, the purpose of this study was to investigate the protective effect of hydrogen on LPS-induced BPD and to explore its potential molecular mechanisms.

Materials And Methods

A neonatal rat model of BPD and administration of hydrogen gas

All experimental procedures were approved by the Experimentation Ethics Committee of Taian City Central Hospital in Shandong, China (permit numbers: 2022-07-10). 8-week-old sprague-dawley (SD) rats were purchased from Shanghai JSJ. Male and female rats with the ratio 2:1 were caged over night, vaginal plugs were confirmed the next morning which was counted as E0.5.

We induced CAM to make a neonatal rat model of BPD by injecting LPS (0.2ug/ul, 5ul) into the amniotic fluid at E16.5. LPS, from Escherichia coli (O55:B5), was purchased from Sigma–Aldrich (L2880, Shanghai, CHINA). Pregnant rats were anesthetized by inhaling 5% isoflurane, and then maintained with 2% isoflurane until the end of induction. Carefully injected 5ul LPS/saline to each amniotic sac after exposed by a midline abdominal aseptic incision and accounted the numbers. Pregnant rats divided into three groups with 5 in each group: intra-amniotic injection of saline as the control (CON group), intra-

amniotic injection of LPS as the LPS group, treatment of 30% hydrogen gas for 4 hour/day with continously 5days upon the intra-amniotic injection of LPS as the LPS + H_2 group.

The placenta and umbilical cord were collected by cesarean section at E21.5 and the weight of neonate and placenta were recorded. The newborn rats were fed with breast-feeding rats prepared in advance. Intrauterine fetal death (IUFD) rate was calculated by the number of stillbirths based on fetal counts at E16.5. The number of surviving pups was continuously counted until postnatal day 14 (P14). The body weights of pups were measured at P0, P7 and P14.

Tissue Preparation

Placenta, umbilical cord and the left lung of rats at P0, P7 and P14 were collected to HE staining and TUNEL apoptotic index analysis subsequently. Pups were euthanized at P7 and P14 by an intraperitoneal injection of 120 mg/kg (2 ml/kg) of sodium pentobarbital, followed by cardiac perfusion with precooled saline. The placenta was placed in the tubes and stored frozen in -80℃ for ELISA, RNA-seq assay.

Hematoxylin-Eosin (HE) staining for histopathology analysis

To intuitively evaluate the degree of LPS-induced CAM and assess the perturbed lung development in different groups, the tissues, including the placentae, umbilical cords and pups' lungs, were paraffin-embedded and sliced at 5mm after fixed with 4% PFA for 24 hours. Then, they were respectively stained with hematoxylin and eosin (H&E; Sigma-Aldrich) to assess inflammatory cell infiltration and lung development. Finally, they were dehydrated and rendered transparent and sealed with neutral gum. Sections were observed under a microscope and photographed. Parameters of alveolarization: the mean linear intercept (MLI), radial alveolar count (RAC) and alveolar wall ratio (alveolar wall area/total area) were measured.

TUNEL staining in lung tissue

We carried out the TUNEL assay through the TUNEL Apoptosis Detection Kit (FITC) (Yeasen Biotechnology (Shanghai), China). The lung slices at P0 and P7 were dewaxed with xylene and rehydrated with alcohol. 20min was treated with protease K at room temperature and washed with PBS for 3 times. After followed by the instructions, the FITC-labeled TUNEL positive cells were imaged under an inverted fluorescence microscope.

RNA sequencing (seq) -RNA extraction, library construction and sequencing

According to the manufacturer's protocol, using Trizol reagent kit (Invitrogen, Carlsbad, CA, USA) extracted the total RNA, then proceeded the assessment of RNA quality on an Agilent 2100 Bioanalyzer (Agilent Technologies, Palo Alto, CA, USA) and checked with RNase free agarose gel electrophoresis. After total RNA was extracted, eukaryotic mRNA was enriched by oligo (dT) beads. Then the enriched mRNA was fragmented into short fragments using fragmentation buffer and reversely transcribed into cDNA by using NEBNext Ultra RNA Library Prep Kit for Illumina (NEB#7530, New England Biolabs, Ipswich, MA,

USA). The purified double-stranded cDNA fragments were end repaired. A base added and ligated to Illumina sequencing adapters. The ligation reaction was purified with the AMPure XP Beads (1.0X). Ligated fragments were subjected to size selection by agarose gel electrophoresis and polymerase chain reaction (PCR) amplified. The resulting cDNA library was sequenced using Illumina Novaseq6000 by Gene Denovo Biotechnology Co. (Guangzhou, China).

RNA seq-bioinformatics analysis

Filtering reads to get high quality clean reads and alignment with both ribosome RNA (rRNA) and reference genome, prepared for further assembly and gene abundance calculation. A FPKM (fragment per kilobase of transcript per million mapped reads) value was calculated to quantify the expression abundance and variations by RSEM software. We calculated the correlation coefficient between two replicas to evaluate repeatability between samples by correlation analysis. To identify the differentially expressed genes, we performed the analysis by the DESeq2 software between two different groups (and by edgeR between two samples). Parameters of the genes/transcripts were considered differentially statistical significance when q-value < 0.05 (the corrected p-values obtained by the BH algorithm) and absolute fold change ≥ 2.

Differentially expressed genes were mapped to GO terms in the Gene Ontology database (http://www.geneontology.org/), gene numbers were calculated for every term, significantly enriched GO terms in DEGs comparing to the genome background were defined by hypergeometric test. Kyoto Encyclopedia of Genes and Genomes (KEGG) pathway enrichment analysis was performed to identify significantly enriched metabolic pathways and signal transduction pathways in DEGs.

ELISA assay

To validate the levels of protein related to TNF-α/NF-κB inflammatory signaling pathway in placenta, we used the ELISA assay to measure the placental protein levels. Accurately weighed placental tissue and rushed with balls at 4°C, and stored overnight at -20℃. Upon two freeze-thaw cycles, the supernate was removed after the homogenates centrifuged at 5000 x g for 5 min at 4℃. Separated the samples to be tested and stored them at-20℃. Protein concentration was determined by BCA protein assay kit (Thermo Fisher Scientific, MA, United States). The contents of TNF-α, NF-κB (p65), interleukin-1β (IL-1β), IL-18, IL-6, IL-10, C-C motif chemokine ligand 2 (CCL2) and C-X-C motif chemokine ligand 1 (CXCL1) in placental tissues were determined by ELISA assay kits, including TNF-α uncoated ELISA kits (Cat.no.88-7340, Thermo Fisher Scientific, MA, United States), IL-6 uncoated ELISA Kit (Cat.no.88-50625, Thermo Fisher Scientific, MA, United States), IL-10 uncoated ELISA Kit (Cat.no.88-50629, Thermo Fisher Scientific, MA, United States), CCL2 ELISA Kit (Cat.no.EK387-96, MULTI Scientific, Hanzhou, China), CXCL1 Elisa Kit (Cat.no.EK396, MULTI Scientific, Hanzhou, China), IL-1β ELISA Kit (Cat.no.SEA563Ra, USCN KIT INC. Wuhan, China), IL-18 ELISA Kit (Cat.no.SEA064Ra, USCN KIT INC. Wuhan, China), and NF-κB (p65) ELISA kits (Cat. no.CSB-E08788r, Cusabio Technology, Wuhan, China).

Statistical analysis

Statistical analysis was performed with GraphPad Prism 8.0 database. All results were presented as mean ± SD, $p < 0.05$ was considered as significant. All data were analyzed using one-way analysis of variance (ANOVA) with the Tukey multiple comparison test. Pearson correlation analysis was used to measure the relationship between NBW and placental weight, the relationship of the levels of proteins TNF-α/NF-κB and the inflammatory factors.

Results

Inhaled hydrogen gas ameliorated LPS-induced BPD in rats

H_2 attenuated the abnormal intrauterine development induced by LPS

The neonatal outcomes results were checked immediately after birth displayed in Table 1. Among the maternal baseline characteristics, the intrauterine fatal death (IUFD) rates were 3/50 (6%) in the CON group, 18/46 (39%) in the LPS group, and 13/48 (27%) in the LPS + H_2 group. Moreover, there was no significant difference of maternal weight and amniotic sacs.

Table 1
The maternal baseline characteristics in different groups.

	CON	LPS	LPS + H_2
Maternal rat (n)	5	5	5
Maternal weight (g)	298.80 ± 7.83	301.00 ± 8.25	285.60 ± 5.44
Gestational sacs (n)	50	46	48
Fetal death (n)	3	18	13
IUFD rate (%)	6	39	27

H_2 inhalation improved the poor outcomes of neonatal rats

Similarly, the pups in LPS group represented a growth-restricted state in the postnatal days in Fig. 1, mainly in the lower body weight at P0-P14 (Fig. 1A) and lower survival rate up to P14 (Fig. 1B). While, the dysplasia and the lower survival ratio were all improved by hydrogen shown in LPS + H_2 group ($p < 0.01$).

Positive correlation between placental weight and BW

Compared with CON group, BW in LPS group was significant lower shown in Fig. 2A. Equally, the average placental weight in LPS group was also at a lower level shown in Fig. 2B. Interestingly, the above abnormalities were improved after inhaling hydrogen ($p < 0.05$). A positive relationship between placental weight and BW was found in pups at P0 ($r = 0.7528$; $p < 0.0001$; Fig. 2C).

H_2 inhalation relieved the LPS-induced BPD

Inhaled H_2 relieved the LPS-induced perturbed lung development

Perturbed lung development with obviously lagging behind was demonstrated in LPS group by histological examination. LPS treatment abnormally increased the alveolar size, resulting in the heterogeneous alveolar and severe inflammatory response with a large number of polymorphonuclear leukocyte infiltration. Fortunately, hydrogen normalized the alveolar sizes, pulmonary septum and evidently reduced the inflammatory cell infiltration (Fig. 3A). Quantitatively, the parameters of alveolarization: the alveolar wall area ratio and MLI were increased by LPS, RAC was decreased by LPS. On the contrary, the above disorder-induced by LPS were normalized by hydrogen (Fig. 3B-D).

Inhaled H_2 mitigated the LPS-induced lung injury

Figure 4 revealed the lung apoptotic index by TUNEL assay. Compared with CON and LPS + H_2 groups, the LPS group owned a highest apoptotic index in lung disrupted by LPS at P0 and P7 (Fig. 4A and Fig. 4C). Quantitatively, H_2 inhalation could protect against the injury from LPS by reducing the apoptosis at P0 and P7 ($p < 0.05$) (Fig. 4B and 4D).

Hydrogen inhalation inhibited the excessive inflammatory response of LPS-induced placenta and fetus

In order to explore the role of H_2 in inhibiting placental inflammatory response, we analyzed the morphology of placental tissue by HE staining to observe the changes of placental inflammation intuitively and evaluate the degree of placental inflammation in CON, LPS and LPS + H_2 groups. Placentae in LPS group were displayed with severe CAM which were manifested as a large number of polymorphonuclear leukocyte infiltration (200×, Fig. 5A), involving the lower pole of the amniotic sac, the intervillous space, the chorionic plate, decidua and even the whole layer of placenta (100×, Fig. 5A). Interestingly, upon administration of H_2, infiltration degree was remarkably reduced and infiltration range significantly narrowed down, only amniotic sac and chorionic plate were involved. Similarly, this phenomenon was also presented in the HE staining of umbilical cord, which reflected the degree of inflammation in the fetus. Unlike the CON group, inflammatory cells were scattered in the umbilical artery (200×, Fig. 5B) and amniotic membrane surrounding (100×, Fig. 5B) in LPS group, but not in LPS + H_2 group. Results were shown in Fig. 5.

TNF-α/NF-κB signaling pathway may be involved in hydrogen inhalation rescue from LPS-induced inflammatory

imbalance in placenta

Alterations in placental mRNA levels of TNF-α/NF-κB signaling pathway relevant proteins

To further verify the underlying mechanisms of H_2 effect, the transcriptome in CON, LPS and LPS + H_2 groups was determined via RNA-seq. Differentially expressed genes in the three groups (CON, LPS and LPS + H_2) indicated that H_2 could take therapeutic effect on the LPS-induced BPD via various molecular mechanisms. A total of 671 genes with significant difference were screened out when comparing LPS + H_2 group with LPS group, including 78 up-regulated and 593 down-regulated genes (Fig. 6A). Significantly enriched GO terms were identified in biological processes, which included the 'inflammatory response' and 'cytokine production' (Fig. 6B). Further digging mechanism, KEGG pathway analysis was also applied to analyze the dysregulated genes involved in various signal transduction pathways. Among the top 20 of KEEG enrichments, TNF signaling pathway was strikingly located (Fig. 6C).

Meanwhile, the mRNA expressions of proteins related to TNF signaling pathway from the different groups were presented as the fpkm levels (Fig. 6D). Compared with the CON group, the results displayed the LPS group owned a higher levels of TNF-α induced protein2 (TNFaip2), TNFaip3 and TNFaip6. Previous studies have revealed that key role of TNF-α in BPD. According to the GO and KEEG analysis in this research, the results revealed that TNF-α/NF-κB-mediated signaling pathway was involved in the inflammatory response. Therefore, it was hypothesized that H_2 may function via the TNF-α/NF-κB signaling pathway. H_2 inhalation could alleviate the up-regulated mRNA levels of TNF-α and NF-κB in LPS group ($p < 0.05$). Similarly, up-regulated mRNA levels of inflammatory cytokines (IL-6, IL-18 and IL-1β) and inflammatory chemokines (CXCL1, CCL2) in LPS group were also remarkably reversed by H_2 inhalation ($p < 0.05$, Fig. 6D), but not in IL-10 ($p > 0.05$).

Alterations in placental protein levels of TNF-α/NF-κB signaling pathway relevant proteins

To evaluate the role of H_2 in the protein of TNF-α/NF-κB signaling pathway in placenta, we conducted the ELISA assay to assess alterations in expression of the key proteins involved in these pathways in CON, LPS and LPS + H_2 groups. Results were demonstrated in Fig. 7.

H_2 inhalation moderated the increased placental proteins levels of TNF-α and NF-κB levels in LPSinduced BPD. Compared to the CON group, the placental protein level of TNF-α in LPS group was remarkably increased in response to LPS ($p < 0.05$; Fig. 7A). In addition, NF-κB(p65), which was detected to reflect the total NF-κB levels, still owned a higher protein level in LPS group ($p < 0.05$; Fig. 7B). Fortunately, inhaled H_2 moderated the above disorder-induced by LPS ($p < 0.05$; Fig. 7A-B).

H_2 inhalation scavenged excessive placental inflammatory cytokines and inflammatory chemokines in LPS-induced BPD. Placenta in LPS group performed the inflammatory storm. For instance, the inflammatory cytokines such as IL-6, IL-18, IL-1β and IL-10 and inflammatory chemokines such as CCL2 and CXCL1 were excessively released by placental cells in response to TNFα based on the Gene enrichment analysis in RNA-seq (Fig. 7C-H). Among them, we identified the significant statistical difference in the IL-6 (Fig. 7C), IL-18 (Fig. 7D), IL-1β (Fig. 7E), CCL2 (Fig. 7G) and CXCL1 (Fig. 7H), but not in IL-10 (Fig. 7F). While, when inhaled H_2 with LPS group, the excessive inflammatory cytokines and chemokines induced by LPS were scavenged ($p < 0.05$). In addition, the protein level of IL-10 was not significantly changed in the three groups (Fig. 7F).

The pivot role of TNF-α/NF-κB signaling pathway in H_2 inhibiting inflammatory response

In order to verify whether H_2 ameliorated LPS-induced BPD through inhibiting the hub protein TNF-α and resulting in down-regulating the NF-κB-mediated the inflammatory response subsequently. We respectively performed pearson correlation analysis on relationship of TNF-α vs both NF-κB(p65) and inflammatory cytokines/chemokines. Our study showed that TNF-α was positively related to NF-κB(p65) protein levels ($p < 0.05$; Fig. 8A). In placenta, both TNF-α and NF-κB(p65) protein expressions were positively associated with inflammatory cytokines (Fig. 8B-G) ($p < 0.05$). A similar relationship was also found between TNF-α/NF-κB(p65) and inflammatory chemokines ($p < 0.05$, Fig. 8H-K).

Discussion

Owing to serious complications and the poor prognosis, BPD has been widely concerned among LPS-induced adverse pregnancy outcomes [19]. BPD, manifested as lung injury, disrupts alveolarization and microvascular development [20]. Intra-amniotic administration of LPS at E16.5 to induce inflammatory cascades-CAM is similar to the major clinical characteristics observed in patients with BPD. CAM can produce excessive inflammatory factors into the fetus, which affect the maturation of fetal lung, cause fetal lung structural remodeling, affect the contractile function of pulmonary vessels, and thus lead to the occurrence of BPD [21, 22]. Our results indicated that LPS group exhibited a disorder of intrauterine development: the intrauterine fatal death (IUFD) rates represented a high level in the LPS group. The surviving newborns also had a lower birth weight and placental weight than those in CON group. Moreover, the results also revealed the poor outcomes of neonatal rats induced by LPS: The pups in LPS group presented a growth-restricted state in the postnatal days, mainly in the lower body weight and lower survival ratio. A perturbed lung development (abnormal alveolarization and severe inflammatory response) was existed in LPS-induced newborn accompanied with obviously lagging behind. Meanwhile, the damaged lung induced by LPS was reflected by a higher apoptotic index. Overall, LPS-induced lung injury reached to model for BPD. Hydrogen gas, a novel therapeutic molecule, the therapeutic potential in anti-apoptotic, anti-oxidative and anti-inflammatory effects has been recognized by many animal studies and clinical trials, especially in lung diseases [23–25]. However, inflammatory scavenging ability is the

widely accepted mechanism of H_2 [26, 27]. In our research, H_2 was incorporated into the treatment of BPD as a therapeutic method. H_2 not only attenuated the abnormal intrauterine development by reducing the IUFD and ameliorating the loss to fetus induced by LPS, but also improved the poor outcomes of neonatal rats through normalizing the LPS-induced perturbed lung development. Our findings indicated that H_2 inhalation was indeed a promising candidate for BPD treatment and the mechanism was deeply excavated in this research.

Recent studies reveal that imbalanced pro-inflammatory and antiinflammatory cytokines in placenta serves a major role in the pathophysiology of BPD, characterized by excessive inflammatory response syndrome which act as exposure risk factor that contribute to the development of BPD[28, 29]. Placental compositions, consisting of cytokines, chemokines and natural antioxidants, have direct consequence to the inflammatory response via anti-inflammatory, anti-bacterial and anti-viral properties [30][31]. It is conceivable that disturbances in placental biochemical composition and in placental signaling pathway contribute to the pathophysiology of BPD. Our results observed the excessive inflammatory response of LPS-induced placenta in rats, the inflammatory cells were scattered in the umbilical artery. Combined with the correlation analysis results (placental weight versus birth weight), there is no doubt that placental dysfunction plays a critical role in the development of BPD.

Previous studies confirm that H_2 can exert anti-inflammatory effects in a variety of cells through multiple signaling pathways. For instance, H_2 can reduce the expression of intercellular adhesion molecules and chemokines to reduce the infiltration of neutrophils and macrophages [32, 33]. In a study of rat burns, H_2 also alleviated the airway inflammatory response by reducing the activation of crucial NF-κB-mediated inflammatory signaling pathway, reducing IL-1β, IL-6 levels subsequently [34]. Currently, Researcher also found the perspectives of H_2 for coronavirus disease-2019 (COVID-19) caused by severe acute respiratory syndrome coronavirus 2 (SARS-CoV-2) [35]. COVID-19 manifested as an acute inflammatory lung injury caused by cytokine storm [36, 37]. H_2 inhalation play notable role in annihilating inflammatory cytokines to inhibit cytokine storm. Due to the remarkably anti-inflammatory effect of H_2, H_2 has been recommended in acute or chronic pulmonary disease to confront COVID-19 pandemic eventually [38]. Our results were consistent with the previous study: H_2 inhalation moderated the excessive inflammatory response of LPS-induced placenta in rats, including reducing the degree of the infiltration and significantly narrowing down the range of infiltration. The fetal inflammatory reaction mitigated upon administration of H_2 equally, reflected by the umbilical artery histology.

BPD has been generally acknowledged as a complicated pathological process, involving complex and redundant molecules and signaling pathways. TNF-α is a major inflammatory messenger, widely involved in inflammation. The activation of TNF-α can initiate the downstream signaling pathway to participate in the development of BPD [39]. As we all known that NF-κB, one of downstream targets activated by TNF-α, can promote inflammatory response, because the transcription of inflammatory factors and the release of these cytokines largely depends on the activation of NF-κB [40]. Given the role of TNF-α and NF-κB signaling pathway relevant proteins to inflammation, we investigated the beneficial effect of inhaled H_2

on LPS-induced BPD, and we raised the question: does hydrogen inhibit inflammation by down-regulating the expression of hub protein TNF-α and subsequently reducing the activity of NF-κB-mediated inflammatory signaling pathway? We identified and evaluated alterations of TNF-α and NF-κB-mediated signaling pathway in placenta of CON, LPS and LPS + H_2 group and the relevant intensity between them. The results demonstrated that H_2 inhalation largely ameliorated the increased mRNA and protein levels of TNF-α and NF-κB (p65) induced by LPS in placenta ($p < 0.05$). Consistently, excessive inflammatory cytokines and chemokines in response to LPS were also scavenged by H_2 inhalation, including IL-6, IL-18, IL-1β, CCL2 and CXCL1. Just as we conceived, the bioinformatics analysis (GO and KEEG analysis) of RNA-seq revealed the prominent role in TNF-α/NF-κB-mediated inflammatory signaling pathway regulated by H_2 inhalation. Proteins, as the messenger of biological function, identifying the relevant intensity of those proteins was conducive to reflect the pivotal role of TNF-α/NF-κB-mediated signaling pathway in regulating the downstream inflammatory cytokines/chemokines. The data confirmed that a positive association of TNF-α versus NF-κB and TNF-α versus inflammatory cytokines/chemokines, was consistent with the role of TNF-α in previous studies. Combining with relevant relationships, we can conjecture that TNF-α contributes to the therapeutic effect of hydrogen inhalation on LPS-induced BPD by regulating the NF-κB-mediated inflammatory signaling pathway, resulting in scavenging excessive inflammatory cytokines and chemokines.

Conclusions

In conclusion, our study demonstrated that H_2 inhalation significantly rescued from LPS-induced BPD, alleviation of LPS-induced BPD by H_2 inhalation was mainly dependent on the inhibition of the TNF-α/NF-κB-mediated signaling pathway, eventually resulting in scavenging inflammatory cytokines/chemokines. However, further research is needed to study the exact mechanism of the H_2 in the pathogenesis of LPS-induced BPD, such as apoptosis, oxidative damages. Larger studies will be required to clarify the role of H_2.

Declarations

Acknowledgements

This study was supported by a grant from the funding of the development Center for Medical Science& Technology National Health Commission of the People's Republic of China (WA2020HK63 to Guo Yao) and Science and Technology Program of Taian, China (2021NS327 to Yafang Zhang); we acknowledge Central Laboratory of Taian City Central Hospital. We are grateful for Shanghai Asclepius Meditec Co., Ltd for their support of hydrogen/oxygen nebulizer.

Conflict of interest

All authors approve the final manuscript and declare no relevant conflicts of interest.

Author contributions

YFZ and XHR drafted the manuscript. LLZ and ZXC analyzed data. GY and YW contributed to concept and designed the study. YFZ, XHR, YXC and YT performed the research. YW and GY revised and made suggestions for final revisions. Guo Yao and YFZ supported the funding of the research. All authors read and approved the final manuscript.

References

1. Schmidt A R, Ramamoorthy C. Bronchopulmonary dysplasia[J]. Paediatr Anaesth, 2022, 32(2):174-180. DOI:10.1111/pan.14365.
2. Gilfillan M, Bhandari A. Diagnosis and management of bronchopulmonary dysplasia[J]. BMJ, 2021, 375:n1974. DOI:10.1136/bmj.n1974.
3. Hwang JS, Rehan VK. Recent Advances in Bronchopulmonary Dysplasia: Pathophysiology, Prevention, and Treatment [J]. Lung, 2018, 196(2): 129-138. DOI:10.1007/s00408-018-0084-z.
4. McGrath-Morrow S A. Bronchopulmonary dysplasia: what are its links to COPD?[J]. Ther Adv Respir Dis, 2019,13:1023339764. DOI:10.1177/1753466619892492.
5. Papagianis P C, Pillow J J, Moss T J. Bronchopulmonary dysplasia: Pathophysiology and potential anti-inflammatory therapies[J]. Paediatr Respir Rev, 2019,30:34-41. DOI:10.1016/j.prrv.2018.07.007.
6. Villamor-Martinez E, Alvarez-Fuente M. Association of Chorioamnionitis With Bronchopulmonary Dysplasia Among Preterm Infants: A Systematic Review, Meta-analysis, and Metaregression[J]. JAMA Netw Open, 2019,2(11):e1914611. DOI:10.1001/jamanetworkopen.2019.14611.
7. Mir I N, Chalak L F. Impact of multiple placental pathologies on neonatal death, bronchopulmonary dysplasia, and neurodevelopmental impairment in preterm infants[J]. Pediatr Res, 2020,87(5):885-891.DOI:10.1038/s41390-019-0715-y.
8. Budal E B, Ebbing C, Kessler J, et al. Placental histology predicted adverse outcomes in extremely premature neonates in Norway-population-based study[J]. Acta Paediatr, 2022,111(3):546-553.DOI:10.1111/apa.16198.
9. McCartney S A, Kapur R. Amniotic fluid interleukin 6 and interleukin 8 are superior predictors of fetal lung injury compared with maternal or fetal plasma cytokines or placental histopathology in a nonhuman primate model[J]. Am J Obstet Gynecol, 2021,225(1):81-89. DOI:10.1016/j.ajog.2020.12.1214.
10. Rallis D, Lithoxopoulou M, Pervana S, et al. Clinical chorioamnionitis and histologic placental inflammation: association with early-neonatal sepsis[J]. J Matern Fetal Neonatal Med, 2021:1-7.DOI:10.1080/14767058.2021.1961727.
11. Goncalves L F, Cornejo P, Towbin R. Neuroimaging findings associated with the fetal inflammatory response syndrome[J]. Semin Fetal Neonatal Med, 2020,25(4):101143. DOI:10.1016/j.siny.2020.101143.

12. Nie C, Ding X. Hydrogen gas inhalation alleviates myocardial ischemia-reperfusion injury by the inhibition of oxidative stress and NLRP3-mediated pyroptosis in rats[J]. Life Sci, 2021,272:119248.DOI:10.1016/j.lfs.2021.119248.
13. Tian Y, Zhang Y, Wang Y, et al. Hydrogen, a Novel Therapeutic Molecule, Regulates Oxidative Stress, Inflammation, and Apoptosis [J]. Front Physiol, 2021,12:789507. DOI:10.3389/fphys.2021.789507.
14. Yang M, Dong Y. Hydrogen: A Novel Option in Human Disease Treatment[J]. Oxid Med Cell Longev, 2020,2020:8384742. DOI:10.1155/2020/8384742.
15. Zhuang X, Yu Y, Jiang Y, et al. Molecular hydrogen attenuates sepsis-induced neuroinflammation through regulation of microglia polarization through an mTOR-autophagy-dependent pathway [J]. Int Immunopharmacol, 2020, 81:106287. DOI:10.1016/j.intimp.2020.106287.
16. Wu Y, Yuan M, Song J, et al. Hydrogen Gas from Inflammation Treatment to Cancer Therapy[J]. ACS Nano, 2019, 13(8):8505-8511. DOI:10.1021/acsnano.9b05124.
17. Cole A R, Raza A, Ahmed H, et al. Safety of inhaled hydrogen gas in healthy mice[J]. Med Gas Res, 2019,9(3):133-138. DOI:10.4103/2045-9912.266988.
18. Cole A R. Safety of Prolonged Inhalation of Hydrogen Gas in Air in Healthy Adults[J]. Crit Care Explor, 2021, 3(10):e543. DOI:10.1097/CCE.0000000000000543.
19. McGrath-Morrow S A. Bronchopulmonary dysplasia: what are its links to COPD?[J]. Ther Adv Respir Dis, 2019,13:1023339764. DOI:10.1177/1753466619892492.
20. Thebaud B, Goss K N, Laughon M, et al. Bronchopulmonary dysplasia [J]. Nat Rev Dis Primers, 2019, 5(1):78. DOI: 10.1038/s41572-019-0127-7.
21. Hillman N H, Kemp M W, Fee E, et al. Budesonide with surfactant decreases systemic responses in mechanically ventilated preterm lambs exposed to fetal intra-amniotic lipopolysaccharide [J]. Pediatr Res, 2021, 90 (2): 328-334. DOI: 10.1038/s41390-020-01267-8.
22. Papagianis P C. The effect of human amnion epithelial cells on lung development and inflammation in preterm lambs exposed to antenatal inflammation[J]. PLoS One, 2021, 16(6):e253456. DOI:10.1371/journal.pone.0253456.
23. Li H, Luo Y. Hydrogen as a complementary therapy against ischemic stroke: A review of the evidence[J]. J Neurol Sci, 2019, 396: 240-246. DOI:10.1016/j.jns.2018.11.004.
24. Ohta S. Molecular hydrogen as a preventive and therapeutic medical gas: initiation, development and potential of hydrogen medicine [J]. Pharmacol Ther, 2014, 144(1):1-11. DOI:10.1016/j.pharmthera.2014.04.006.
25. Qi B, Yu Y, Wang Y. Perspective of Molecular Hydrogen in the Treatment of Sepsis[J]. Curr Pharm Des, 2021,27(5):667-678. DOI:10.2174/1381612826666200909124936.
26. Alwazeer D, Liu F F, Wu X Y, et al. Combating Oxidative Stress and Inflammation in COVID-19 by Molecular Hydrogen Therapy: Mechanisms and Perspectives[J]. Oxid Med Cell Longev, 2021,2021:5513868. DOI:10.1155/2021/5513868.

27. Heneau A, Guimiot F, Mohamed D, et al. Placental Findings and Effect of Prophylactic Hydrocortisone in Extremely Preterm Infants[J]. Pediatrics, 2018,141(2). DOI:10.1542/peds.2017-1788.
28. Matsuura H, Matsumoto H, Okuzaki D, et al. Hydrogen Gas Therapy Attenuates Inflammatory Pathway Signaling in Septic Mice[J]. J Surg Res, 2021,263:63-70. DOI:10.1016/j.jss.2021.01.022.
29. Kim C J, Romero R, Chaemsaithong P, et al. Chronic inflammation of the placenta: definition, classification, pathogenesis, and clinical significance[J]. Am J Obstet Gynecol, 2015,213(4 Suppl):S53-S69. DOI:10.1016/j.ajog.2015.08.041.
30. Kim C J, Romero R. Acute chorioamnionitis and funisitis: definition, pathologic features, and clinical significance [J]. Am J Obstet Gynecol, 2015, 213 (4 Suppl): S29-S52. DOI:10.1016/j.ajog.2015.08.040.
31. Cookson M W. Antenatal Vitamin D Preserves Placental Vascular and Fetal Growth in Experimental Chorioamnionitis Due to Intra-amniotic Endotoxin Exposure[J]. Am J Perinatol, 2018,35(13):1260-1270.DOI:10.1055/s-0038-1642033.
32. Chen M. Hydrogen protects lung from hypoxia/re-oxygenation injury by reducing hydroxyl radical production and inhibiting inflammatory responses[J]. Sci Rep, 2018, 8(1):8004. DOI:10.1038/s41598-018-26335-2.
33. Zhao S, Mei K. Therapeutic effects of hydrogen-rich solution on aplastic anemia in vivo [J]. Cell Physiol Biochem, 2013,32(3):549-560. DOI:10.1159/000354459.
34. Wang X, Yu P, YongYang. Hydrogen-rich saline resuscitation alleviates inflammation induced by severe burn with delayed resuscitation [J]. Burns, 2015,41(2):379-385. DOI:10.1016/j.burns.2014.07.012.
35. Wang ST. Hydrogen gas (XEN) inhalation ameliorates airway inflammation in asthma and COPD patients [J]. QJM, 2020, 113(12):870-875. DOI:10.1093/qjmed/hcaa164.
36. Fara A, Mitrev Z. Cytokine storm and COVID-19: a chronicle of pro-inflammatory cytokines[J]. Open Biol, 2020, 10(9):200160. DOI:10.1098/rsob.200160.
37. Ye Q, Wang B, Mao J. The pathogenesis and treatment of the `Cytokine Storm' in COVID-19[J]. J Infect, 2020,80(6):607-613.DOI:10.1016/j.jinf.2020.03.037.
38. Guan W J, Chen R C. Strategies for the prevention and management of coronavirus disease 2019[J]. Eur Respir J, 2020,55(4). DOI:10.1183/13993003.00597-2020.
39. Ren Z, Mo W, Yang L, et al. Cord blood antimicrobial peptide LL37 levels in preterm neonates and association with preterm complications [J]. Ital J Pediatr, 2022, 48(1):111. DOI: 10.1186/s13052-022-01295-6.
40. Caire R, Dalix E. YAP Transcriptional Activity Dictates Cell Response to TNF In Vitro[J]. Front Immunol, 2022, 13:856247. DOI:10.3389/fimmu.2022.856247.

Figures

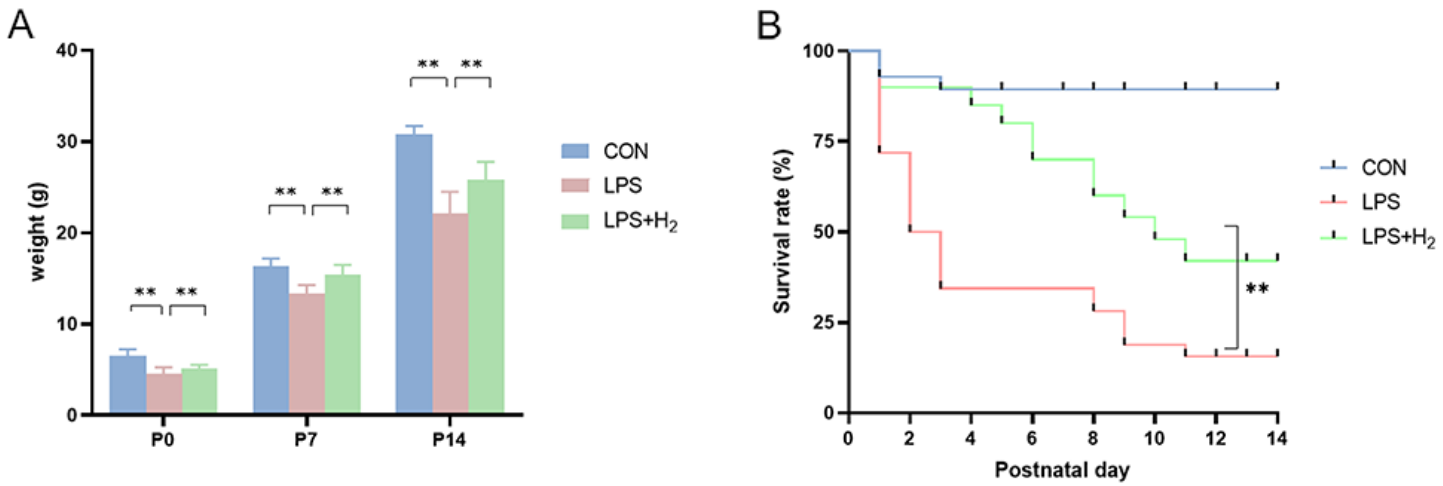

Figure 1

The outcomes of neonatal rats dynamically from P0 to P14. (A) Body weights of pups at P0 (n=15 for CON, 15 for LPS, and 15 for LPS+H_2) and P7 (n=15 for CON, 12 for LPS, and 15 for LPS+H_2) and P14 (n=12 for CON, 9 for LPS, and 12 for LPS+H_2). Data were presented as mean ± SD using ANOVA analysis followed by Tukey multiple comparison test. *p<0.05, **p<0.01 vs LPS group. (B) Kaplan-Meier survival curves of pups from P0 to P14 (n = 47 for CON, 28 for LPS and 35 for LPS+H_2). Significant difference was observed by the log-rank test (p = 0.0017).

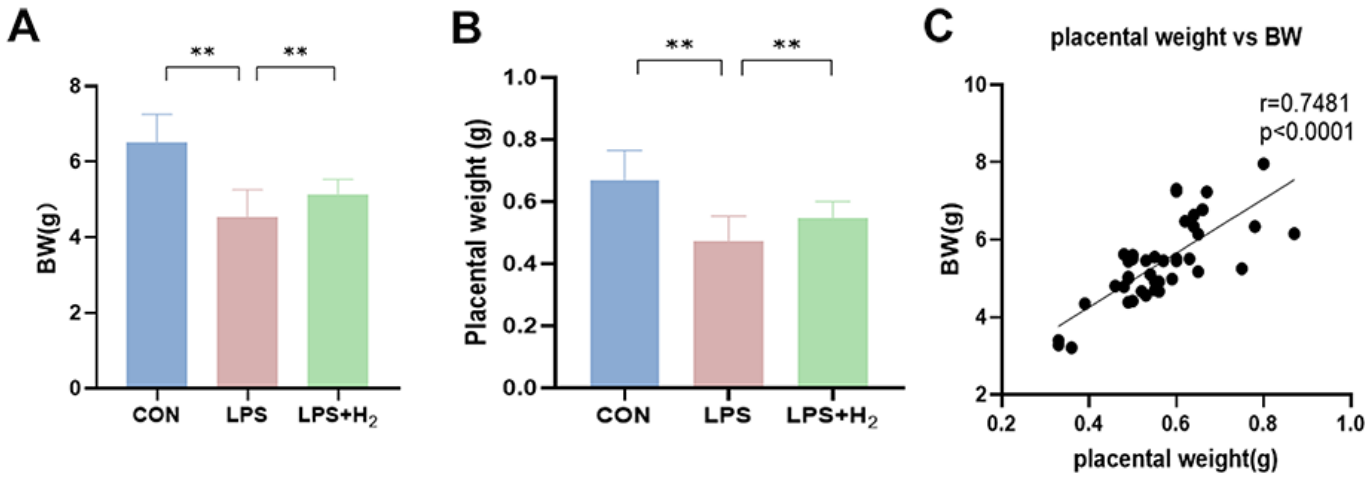

Figure 2

The neonatal baseline characteristics in CON, LPS and LPS+H_2 groups. (A-B) Birth weight (BW) and placental weight of pups (a total of 15 newborn rats were selected from each group (3 newborns were randomly selected from each maternal rats); n=15 for CON, 15 for LPS and 15 for LPS+H_2). *p<0.05, **p<0.01 vs LPS group. (C) Relationship between BW and placental weight in all groups (n = 45), r = Pearson's correlation coefficient.

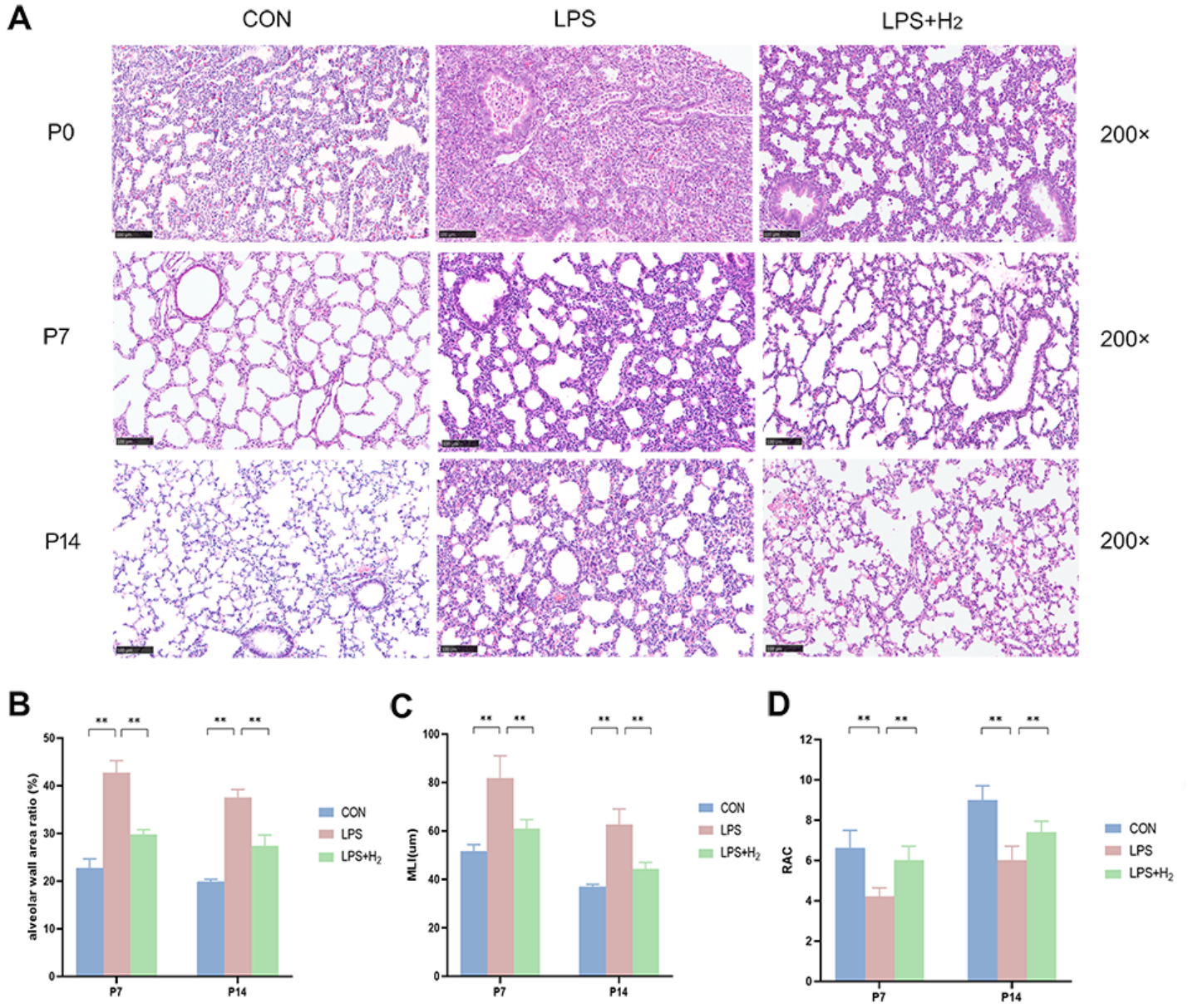

Figure 3

The lung pathological histology in CON, LPS and LPS+H_2 groups. (A) HE staining of lung tissues at P0, P7 and P14 (scale bar, 100um). (B) The alveolar wall area ratio: using the Image J software to quantitatively calculate the alveolar wall area and total area, then calculate the ratio to analyze the statistical difference in the three groups (n=5). (C-D) Respectively, graphic representation of abundance of average of mean linear intercept (MLI) and radial alveolar count (RAC) at P7 and P14 in three groups (n=5). *p<0.05, **p<0.01 vs LPS group.

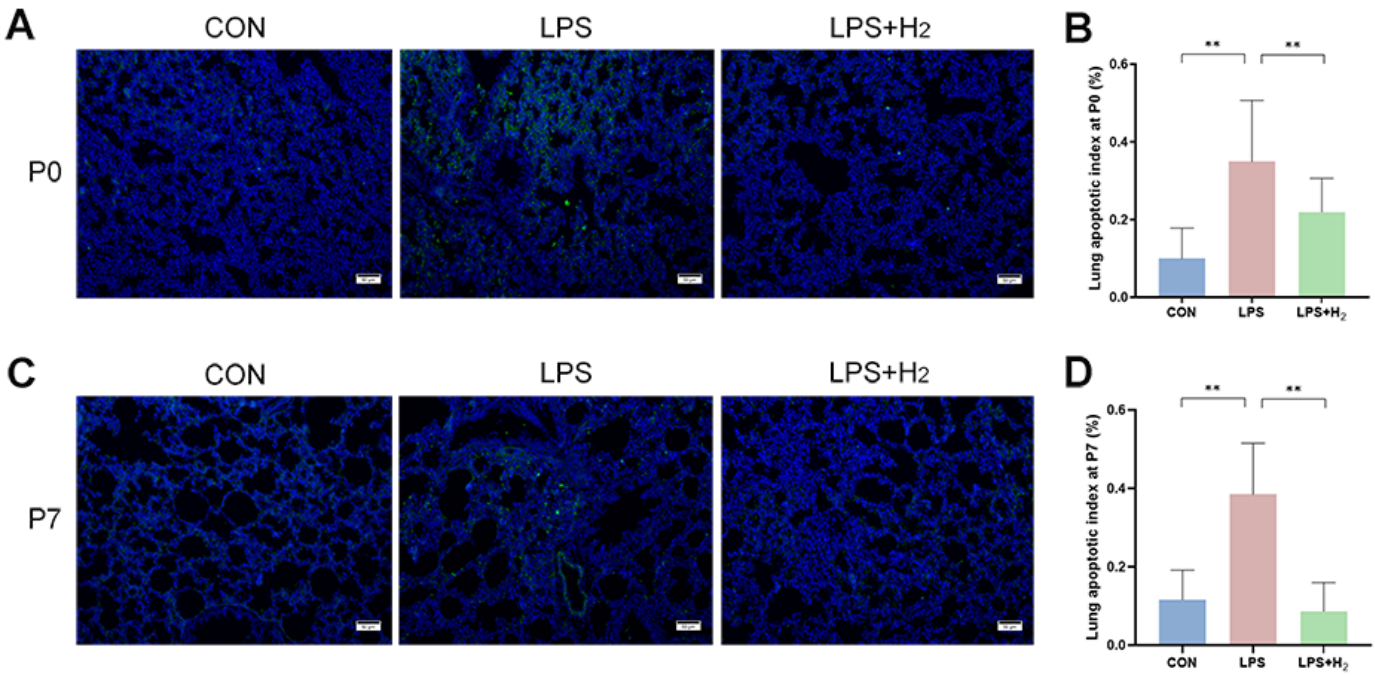

Figure 4

The lung apoptotic indexes at P0 and P7 in different groups by TUNEL assay (200×). (A, C) TUNEL staining of CON, LPS and LPS+H_2 lungs at P0 (A) and P7 (C). (B, D) Average of lung apoptotic index at P0 (B) and P7 (D) (n=5). *p<0.05, **p<0.01 vs LPS group.

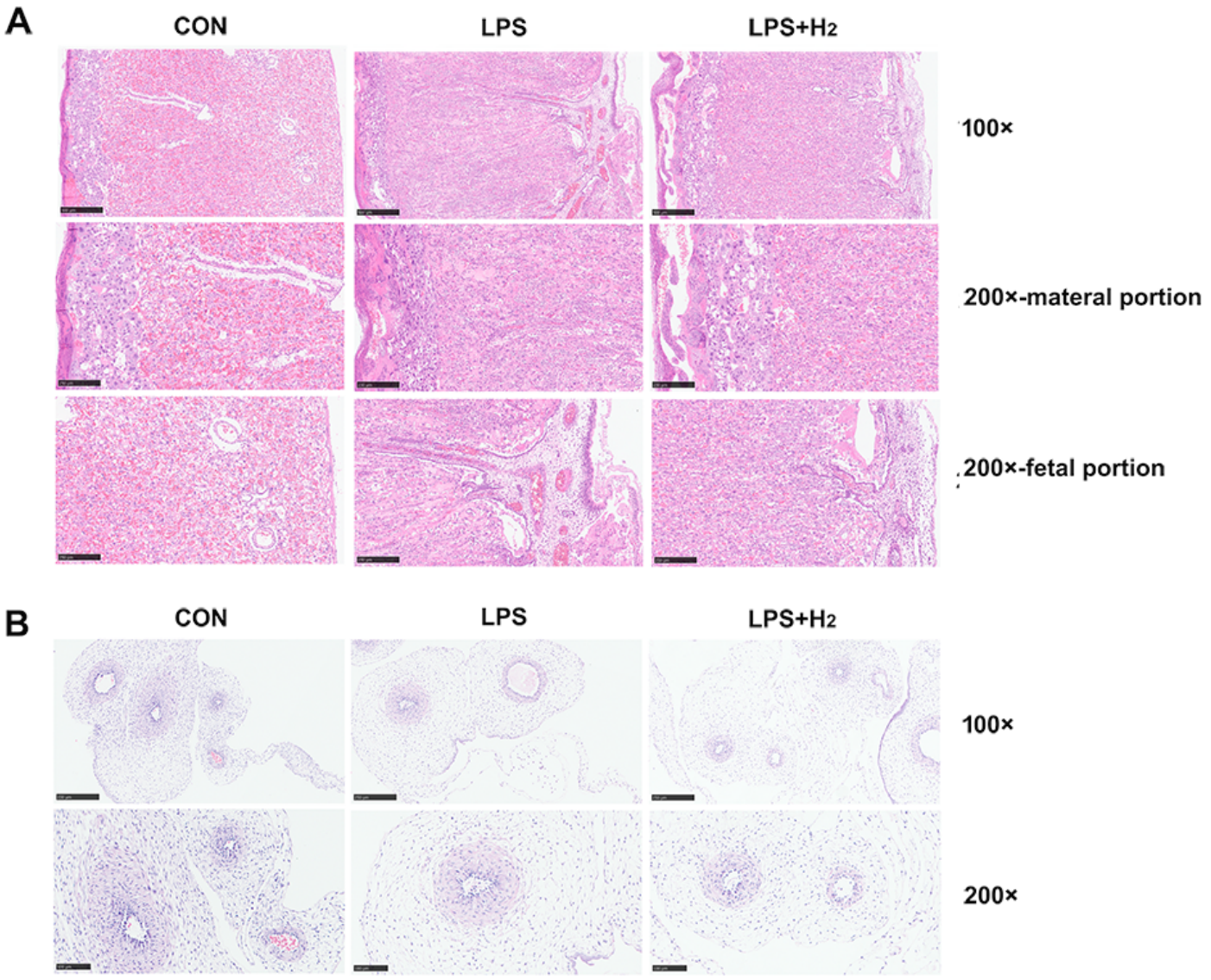

Figure 5

Placental and umbilical cord histologies by HE staining in CON, LPS and LPS+H_2 groups. (A) Histology of placenta in CON, LPS and LPS+H_2 groups. 100× images showed the whole layer of placenta, 200× images showed the maternal portion and fetal portion to present the degree of polymorphonuclear leukocyte infiltration. (B) Histology of umbilical cord in CON, LPS and LPS+H_2 groups.

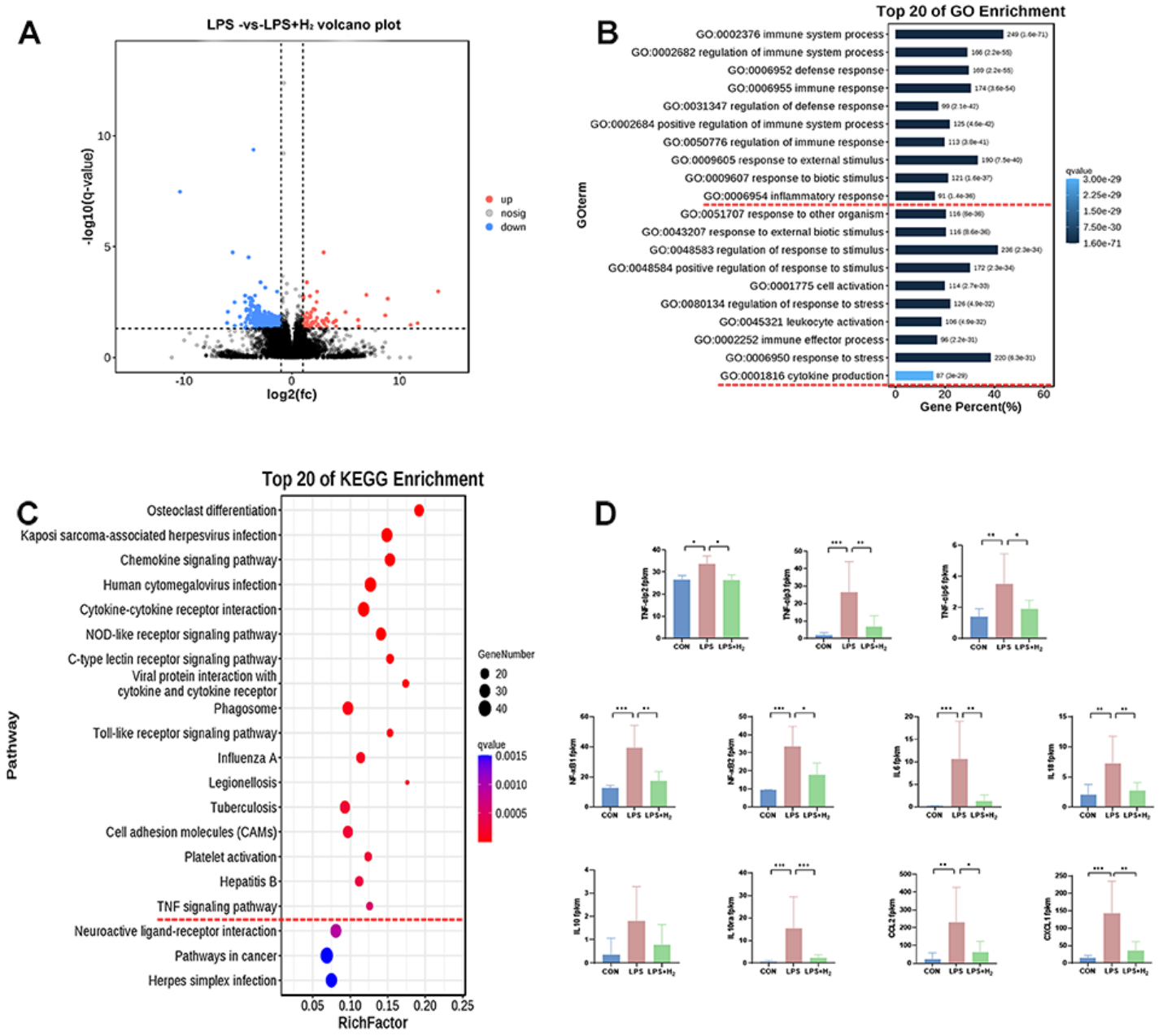

Figure 6

Hydrogen reversed the dysregulated placental mRNA of the TNF-α/NF-κB signaling pathway in response to LPS. (A) Placentae in the LPS group and LPS+H_2 group were sent for RNA sequencing. A volcano plot map of the differentially expressed genes was identified with cut-off values of q-value < 0.05 and |log(fc)| >1, in which red represented up-expression and blue represented down-expression. (B, C) GO and KEEG enrichment analysis were performed with the differentially expressed genes. (D) The fpkm levels were used to represented the dysregulated mRNA levels of the TNF-α/NF-κB signaling pathway which were induced by LPS and reversed by H_2 treatment (n=4). *p<0.05, **p<0.01, ***p<0.001 vs LPS group, q-value: the corrected p-values obtained by the BH algorithm was conceptually equivalent to adjusted p-value,

TNFaip2: TNF-α induced protein 2, NF-κB1: nuclear factor kappa B subunit 1, IL-6: interleukin 6, CCL2: C-C motif chemokine ligand 2, CXCL1: C-X-C motif chemokine ligand 1.

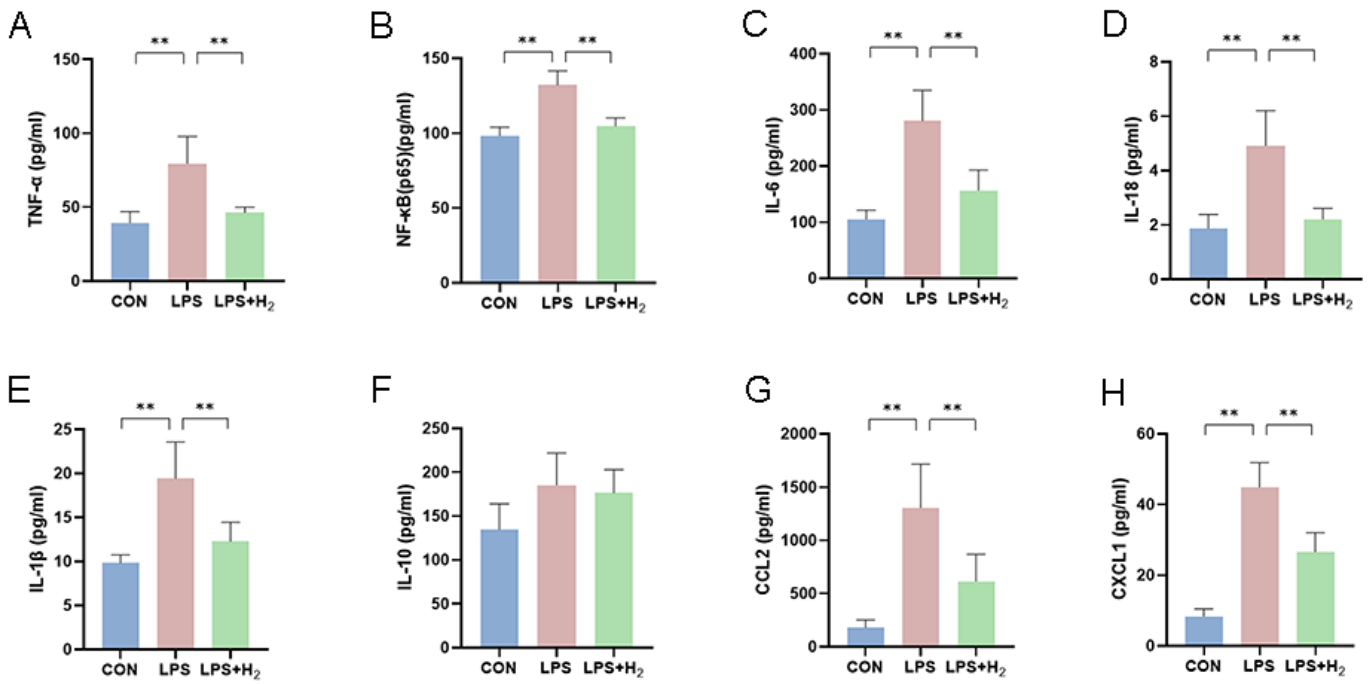

Figure 7

H_2 relieved the excessive inflammatory cytokines and chemokines in LPS-induced BPD detected by ELISA assay.(A-H) Protein levels of TNF-α, NF-κB(p65), IL-6, IL-18, IL-1β, IL-10, CCL2 and CXCL1 in placenta (n=5). *p<0.05, **p<0.01 vs LPS group.

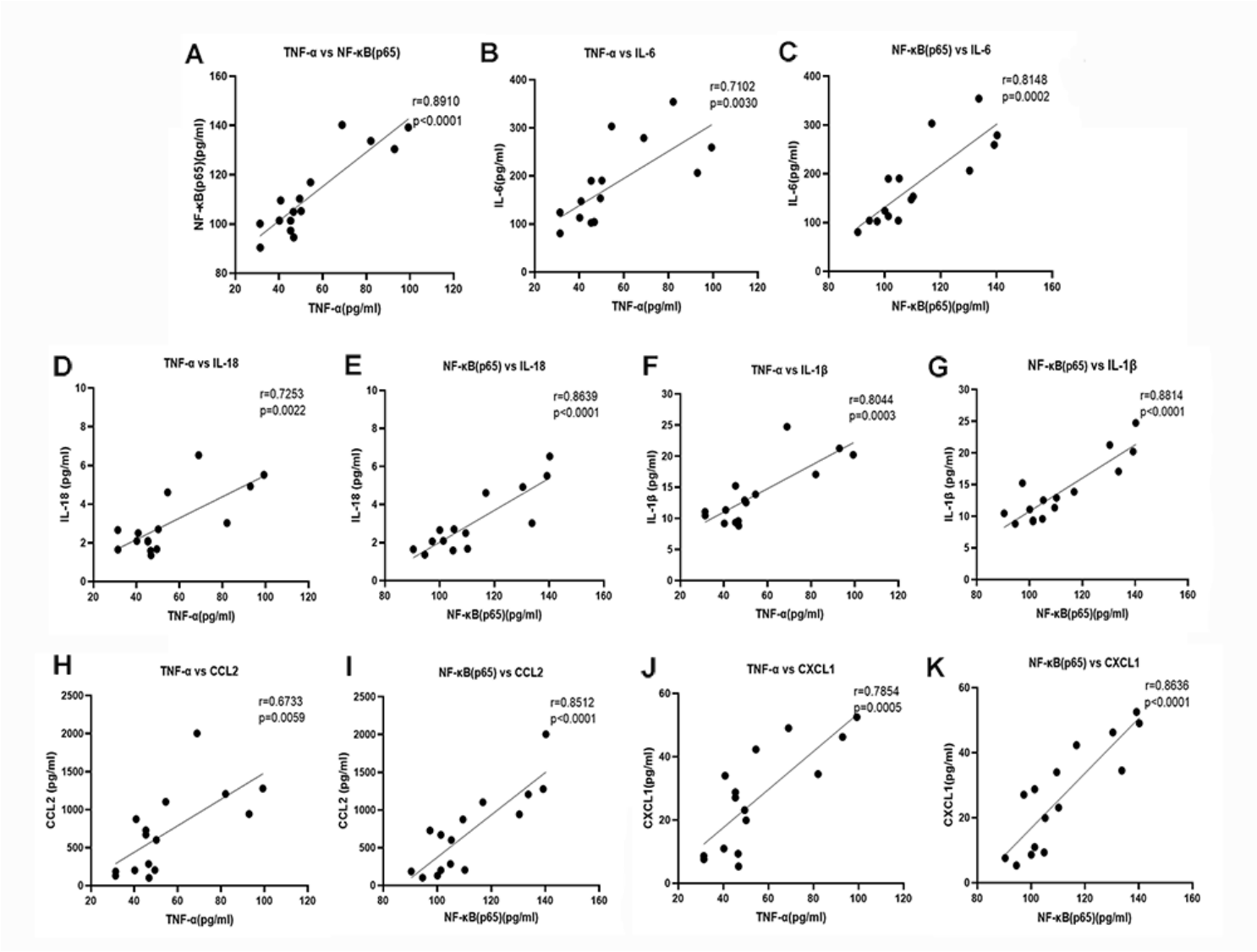

Figure 8

The relationships of between TNF-α/NF-κB(p65) and protein levels of inflammatory cytokines/chemokines in placenta from the three groups. (A) Relationship between TNF-α and placental NF-κB(p65) protein levels in all groups; (B-C) TNF-α vs IL-6 and NF-κB(p65) vs IL-6; (D-E) TNF-α vs IL-18 and NF-κB(p65) vs IL-18; (F-G) TNF-α vs IL-1β and NF-κB(p65) vs IL-1β; (H-I) TNF-α vs CCL2 and NF-κB(p65) vs CCL2; (J-K) TNF-α vs CXCL1 and NF-κB(p65) vs CXCL1; n=15, r = Pearson's correlation coefficient.

Supplementary Files

This is a list of supplementary files associated with this preprint. Click to download.

- S2Fig.EthicsStatement.tif